Transverse Collective Beam Forces and Self-Inflection of a Relativistic Electron Beam in Axisymmetric Magnetic Fields

I. Hofmann, A.U. Luccio[+], and C.E. Nielsen[++]

IPP 0/26

December 1974

MAX-PLANCK-INSTITUT FÜR PLASMAPHYSIK

GARCHING BEI MÜNCHEN

MAX-PLANCK-INSTITUT FÜR PLASMAPHYSIK

GARCHING BEI MÜNCHEN

Transverse Collective Beam Forces and Self-Inflection of a Relativistic Electron Beam in Axisymmetric Magnetic Fields

I. Hofmann, A.U. Luccio[+], and C.E. Nielsen[++]

IPP 0/26 December 1974

[+]Istituto di Scienze dell'Informazione, Universitâ di Pisa, Italy

[++]Department of Physics, The Ohio State University, Columbus, Ohio, U.S.A.

Die nachstehende Arbeit wurde im Rahmen des Vertrages zwischen dem Max-Planck-Institut für Plasmaphysik und der Europäischen Atomgemeinschaft über die Zusammenarbeit auf dem Gebiete der Plasmaphysik durchgeführt.

IPP 0/26

I. Hofmann
A.U. Luccio
C.E. Nielsen

Transverse Collective Beam Forces and Self-Inflection of a Relativistic Electron Beam in Axisymmetric Magnetic Fields

December 1974

Abstract

The results of an analytical and numerical study of some effects of collective fields upon transverse oscillations of a REB in an axisymmetric magnetic field are presented. Intra-beam and beam-beam effects in multiturn systems are included and the various forms of space charge induced coupling investigated. The situation described here is relevant to the first revolutions after injection of intense beams. Special account is given to self-inflection of a REB in an Electron Ring Accelerator.

A Introduction

In this report we present the results of analysis and numerical computation of some effects of collective fields upon the transverse oscillations of intense beams moving in an axisymmetric magnetic field. We consider primarily beams with substantial coherent transverse motion, as is present at injection during beam inflection and capture. The immediate motivation for this work was the observation of collective phenomena during beam injection in Electron Ring Accelerator experiments. The results will, however, be applicable also to other cases in which a beam has coherent transverse oscillations, as may for example develop from growth of an instability such as the resistive wall instability or the trapped charge coupling instability.

It has long been known that capture of charged particles into closed orbits in magnetic fields, either constant or slowly varying, can be significantly influenced by particle space charge. The existence of space charge effects is manifested by a non-linear dependence of captured beam upon current injected, and in some cases by capture of appreciable beam without the use of an imposed time-varying inflection field.

Various collective effects have been suggested as of possible importance in the inflection process. One that Kerst [1] considered in connection with early betatron experiments was the change of magnetic guide fields produced by the injected electron beam.

Samoilov and Sokolov [2] observed electron capture into a fixed-field betatron. This now seems to be almost certainly the direct consequence of azimuthal clustering from negative mass effects. (The authors did not advance this explanation of their observation.)

In the present report we restrict ourselves to consideration of the influence of transverse collective beam forces upon betatron oscillations about a fixed equilibrium orbit. We exclude the influence of wall images, of the time-varying inflector field, of time variations in the main guide field, and of possible coupling to azimuthal motion. By making these exclusions we obtain results that exhibit clearly the importance of beam space charge alone in modifying the transverse oscillations. For application to an actual experiment it may be necessary to extend the numerical computations to include image forces and time-varying applied fields.

Initially we considered only radial oscillations. Axial motion, taken to be uncoupled and of constant amplitude, was not included except through its effect on the beam charge distribution. We explored this one dimensional problem analytically using a simple rough approximation, and solved it numerically by following the motion of phase boundaries in r-p_r phase space (1D-BOUNDARY MODEL). A brief summary of some of these one dimensional numerical results has already been published as part of a general review on the Garching ERA experiment [3]. Subsequently we have studied in some detail the effect of coupling to z-oscillations by following numerically the two dimensional motion of assemblies of interacting macroparticles (2D-PARTICLE MODEL). This work is described here in the sequence in which it was done. In Section B we outline the problem and formulate the approximate analysis that indicates the potential importance of transverse beam fields. We develop also some general theoretical background. In Section C we present the computational results. Finally in Section D we discuss the limitations of the models used and the significance of the results. Some of the computational details are given in the appendix.

B Analysis

Historically the first effect of the internal transverse beam field to be calculated was the shift of the individual particle betatron frequencies [4)5)6)]. We are primarily concerned with entirely different phenomena that follow from the exchange of oscillation energy between individual particles or assemblies of particles. All of the results that we obtain for the change in phase space configuration of one beam and the even larger effects of interaction between two beams are simply the consequence of energy exchanges between multiply coupled oscillators.

An exploration of transverse beam coupling was first carried out here four years ago for two interacting beams treated as parallel rigid charge cylinders. It was found then that the force between two 100 A beams in the Garching ERA experiment was adequate to transfer substantial radial oscillation energy in only a few cycles, and this interaction could therefore influence particle trapping.

1. Phase Space Distributions

The one dimensional periodic motion of an assembly of particles is most conveniently described in an appropriate phase space.

Following standard practice, we represent the one dimensional radial configuration of the beam by a distribution $f\ (r,\ p_r)$ in a two dimensional r-p_r phase space. With fluctuations from short range forces and coupling to other degrees of freedom excluded, the function f satisfies the Liouville-Vlasov equation $\frac{df}{dt} = 0$, phase density in the vicinity of any phase point remaining constant in time. In particular, if f is initially a positive constant within some arbitrary phase boundary and zero elsewhere, the system is uniquely defined by the configuration of the phase boundary and the enclosed area is invariant in time. Such a sharp-edged distribution may be a rather good approximation to the actual distribution in many particle beam situations in which the phase area is limited by apertures and physical walls. It is used in that part of the present work concerned with radial motion assumed uncoupled to axial motion.

When a uniform density phase space distribution is bounded by a phase orbit, which implies for a linear force law that the phase area is centered on the equilibrium point, it constitutes a stationary state.

If the motion in the two degrees of freedom is uncoupled, then points in each of the two separate phase planes move so as satisfy Liouville-Vlasov equations and maintain both separate phase areas invariant. The motion can, however, remain uncoupled in the presence of space charge only if each phase space distribution separately constitutes a stationary state, and if charge distribution in the r-z plane is such as to introduce no coupling.

It must be kept in mind that the two component phase plane distribution taken together do not uniquely specify a state for the system, and in particular they do not determine the charge distribution in the r-z plane.

One case commonly analysed [7] is the one in which the beam has elliptical cross section and is of uniform density in physical space. In this case the space charge force increases linearly with distance from the center of the beam and it introduces no coupling between the two components of transverse motion. The only effect of the space charge force is to change the oscillation frequencies, to reduce them if the beam contains no neutralizing trapped particles of charge opposite to that of the beam particles. The usual "space charge limit" is the calculated beam current that ould shift the oscillation frequencies enough to cause loss of particles as the result of an accelerator resonance.

Within this limit the motion in the two separate phase planes remains essentially uncoupled, and with adiabatic variation of external focussing or of space charge forces, stationary states remain stationary states despite change in the shap e of the beam cross-section and of the boundary orbits describing the distribution in the separate planes. A uniform density distribution of elliptical cross section in space, togehter with elliptically bounded uniform phase density stationary distributions in the separate phase planes, is obtained from a uniform surface density of points on a constant energy surface in four dimensional hyperspace. Then the distribution function f becomes

$$f(r, p_r, z, p_z) \sim \delta(E - E_0)$$

with

$$E = 1/2m\,(p_r^2 + p_z^2) + 1/2\, k_r^2 r^2 + \tfrac{1}{2} k_z^2 z^2$$

(The k_r and k_z include the space charge potential and are separable for the postulated uniform density elliptical beam.)

This, the well-known microcanonical distribution, does not necessarily correspond closely to any realizable experimental beam. In particular it imposes an energy correlation upon the motion in the two degrees of freedom requiring particles with maximum oscillation amplitude in one component to have zero amplitude in the other, so that all particles have equal total oscillation energy.

2. Linear Decomposition of Coherent Dipole Mode

The simplest non-stationary state of a beam to deal with is the one produced by the imposition of coherent oscillations on the entire beam in one or both degrees of freedom. A coherent oscillation sometimes referred to as a dipole mode is an oscillation in which the shape of the beam cross-section is unchanged. It is easy to show that with linear external focussing forces such an oscillation may be treated as independent of all other motion of beam particles relative to the mean coordinates of the beam, whether this other motion be stationary or non-stationary. The total motion of any particle is therefore decomposable into the sum of the motion of the center of gravity and the motion of that particle relative to the center of gravity.

This decomposition theorem, analogous to the similar theorem for the planar motion of points in rigid bodies, follows immediately from the equation of motion of a beam particle. Consider the case in which the coherent oscillation of a beam is radial. We may denote the displacement of the ith particle from the equilibrium orbit r_o by $x_i = r_i - r_0$
and write the equation of motion

$$m\ddot{x}_i = F_i$$

Let $x_i = x + u_i$, $x = N^{-1}\sum x_i$, $\sum u_i = 0$

Write $F_i = -k_0(x + u_i) + C(u_i, w_i)$ (w_i is the z particle coordinate relative to the center of mass)

The total force is the sum of the linear external force characterized by k_o and an internal collective force described by the arbitrary function $C(u_i, w_i)$. Since $C(u_i, w_i)$ is composed of equal and opposite force pairs between particles, $\sum C(u_i, w_i) = 0$.
If we put the value for F_i into the euqation of motion and sum over all particles we get

$$m\ddot{x} = -k_0 x$$

The center of mass oscillates at the frequency determined by the external force constant. The beam coherent frequency is the same as the single particle frequency without space charge.

Next after subracting the terms mx = $-k_o x$ from the complete equation we have

$$m\ddot{u}_i = -k_0 u_i + C(u_i, w_i)$$

For the arbitrary collective force function $C(u_i, w_i)$ every particle has a different frequency and there is internal coupling between the two degrees of freedom. At present we are most interested in uniform elliptical cross-section beams for which the two degrees of freedom are decoupled and $C(u_i, w_i) = k_1 u_i$. Then the equation of motion is:

$$m \ddot{u}_i = -(k_0 - k_1) u_i$$

The individual particle motion relative to the center of mass is in this case characterized by one "incoherent frequency", reduced below the single particle frequency by the mutual repulsion. Despite its elementary character (or perhaps because of it) the demonstration that the coherent motion is independent of beam internal behaviour, however non-stationary, is very helpful in facilitating the understanding of the beam-beam interactions that we have studied numerically.

3. Oscillation Frequency of a Quadrupole Mode

Beams that are non-stationary because the phase space boundaries do not lie on particle orbits are characterized by additional frequencies. If the non-stationary boundary of a given beam in one phase plane is an ellipse not too different from the stationary state ellipse, it can be shown that the non-stationary ellipse rotates in the phase plane with a frequency intermediate between the coherent frequency and the incoherent frequency defined in the preceding section. The resulting oscillation of beam cross section, observable at a frequency twice the phase space ellipse rotation frequency, is referred to as a quadrupole mode. In principle such an oscillation can transfer energy by parametric coupling to the other degree of freedom, but this energy transfer will be small unless the two quadrupole frequencies are nearly equal, as with a beam of nearly circular cross-section in a magnetic field of index n close to 0.5.

The frequency of the beam quadrupole oscillation - viewed in the phase plane as a consequence of rotation of the boundary ellipse - can be obtained simply from the condition that individual particle energy variations occur at the rate consistent with the rate at which the time varying field does work on boundary particles.

For simplicity of representation we scale the momentum so that the stationary orbit in the x-p_x plane is circular and of radius a. The non-stationary state is an ellipse of axes $a_0 \pm a_1$ with $a_1 \ll a_0$. Phase motion in the z-p_z plane is stationary with amplitude b_0 and regarded as decoupled from the x-motion. (This requires the two frequencies to be substantially different and incommensurate.)

The beam cross-section is then of uniform but time varying density within the time varying ellipse

$$(x/a)^2 + (z/b_0)^2 = 1$$

As a preliminary to calculating the rotation rate of the non-stationary boundary, we note that so long as the boundary remains elliptical, i.e. so long as it does not develop higher harmonic deviations from the stationary state circle, the amplitude a must remain constant. This constancy is required, given the postulative independence from z-motion, by conservation of total energy and phase area. Total energy is proportional to the second moment of the area, $m_2 = \int \varrho^2 dA$ and with constant total area the second moment determines a uniquely.

The potential of a relativistic beam of uniform charge density within a long elliptical cylinder is

$$\phi = -1/\gamma^2 \, \frac{2\pi\varrho}{a+b}\left(bx^2 + ay^2\right)$$

In the present case charge per unit length $\lambda = \varrho\pi ab$ is const., and

$$\phi = -1/\gamma^2 \, \frac{2\lambda}{ab(a+b)}\left(bx^2 + ay^2\right)$$

If $b = b_o$ and $a = a_o - a_1 \cos 2w_x' t$ then

$$\frac{\partial\phi}{\partial x} \approx -\frac{1}{\gamma^2}\frac{4\lambda x}{a_o(a_o+b_o)}\left[1+\left(\frac{a_1}{a_o}+\frac{a_1}{a_o+b_o}\right)\cos 2w_x' t\right]$$

The calculation of particle frequency ω_x includes the constant term $4\lambda/\gamma^2 a_o(a_o+b_o)$ in the space charge field, and we substract this to leave the periodic term

$$E_p = \frac{4g\lambda x a_1}{\gamma^2}\cos 2w_x' t \quad , \quad g \equiv \frac{1}{\gamma^2}\frac{2a_o+b_o}{a_o^2(a_o+b_o)^2}$$

This field does work on the particle of charge q at $x = \rho \sin(\omega_x t+\delta)$ at the rate

$$\frac{dW}{dt} = Fv = \frac{4g\lambda q a_1}{\gamma^2}\cos 2w_x' t\, \rho \sin(\omega_x t+\delta)\rho\, \omega_x \cos(\omega_x t+\delta)$$

$$= \frac{4g\lambda q a_1 \rho^2}{\gamma^2}\cos 2w_x' t \sin 2(\omega_x t+\delta)$$

Initially when $t = 0$, $\frac{dW}{dt}$ is positive and has its maximum value for $\delta = 45^o$, and it has maximum negative value for $\delta = -45^o$. Integration over a complete period with $\omega_x' \approx \omega_x$ gives the same result. Furthermore all boundary particles from 0 - 90° ahead of the ellipse major axis gain energy and all 0 - 90° behind lose. This radial motion of boundary particles constitutes a boundary wave that travels forward relative to the particles themselves, in effect turning the elliptical configuration at an angular velocity ω_x' exceeding the angular velocity ω_x of the particles.

We now calculate the relation between ω_x and ω_x' from the condition that a particle goes from minimum to maximum energy when relative to the ellipse it moves from the end of the minor axis to the end of the major axis. With k_o and k_1 defined as in the preceding section, the energy increase is

$$\Delta W = \tfrac{1}{2}(k_o - k_1)\left[(a_o+a_1)^2 - (a_o-a_1)^2\right]$$

$$= 2a_o a_1 (k_o - k_1)$$

This increase is equal to the integral of $\frac{dW}{dt}$ over the time from $t = 0$ until $(\omega_x' - \omega_x)t = /2$. The value of δ is $\pi/2$ to correspond to minimum initial particle energy.

Since $a_1 \ll a_0$, we may replace the variable particle amplitude ρ by a_0. Then

$$\Delta W = -2 g \lambda q a_0^2 a_1 w_x \int_{t=0}^{\pi/2(w_x'-w_x)} \cos(2w_x' t) \sin(2w_x t)\, dt$$

If we set $w_x' - w_x = \alpha$, the integral can be written

$$I = -\int_{t=0}^{\pi/2\alpha} \cos(2w_x' t)\left[\sin(2w_x' t)\cos(2\alpha t) - \cos(2w_x' t)\sin(2\alpha t)\right] dt$$

Since $w_x' \gg \alpha$, it is a sufficiently good approximation to replace $\cos(2w_x' t)\sin(2w_x' t)$ by its average value, which is 0, and $\cos^2 2w_x' t$ by its average value, which is 1/2. (The integral can in fact be done exactly if $w_x' = n\alpha$.)

$$I \approx \frac{1}{2} \int_{t=0}^{\pi/2\alpha} \sin 2\alpha t\, dt = \frac{1}{2\alpha}$$

Then

$$g \lambda q\, a_0^2 a_1 w_x/\alpha = 2 a_0 a_1 (k_0 - k_1)$$

Since $w_{0x}^2 = k_0/m$, $w_x^2 = (k_0 - k_1)/m$, $k_1 = \dfrac{4\lambda q}{a_0(a_0+b_0)}$

we have

$$(w_{0x}^2 - w_x^2)\frac{2a_0+b_0}{2(a_0+b_0)} w_x/\alpha = 2 w_x^2$$

independent of amplitude a_1.

In a beam of circular cross-section $a_o = b_o$ and we obtain, writing all frequencies in units of the gyro-frequency $\Omega = v_\varphi/R$

(B.1.1) $$\alpha/\nu_x = 3/16\left(\nu_{0x}^2/\nu_x^2 - 1\right)$$

For completeness we add the standard formulae for the space charge shifted incoherent betatron frequencies

(B.1.2) $$\nu_x \equiv \frac{w_x}{\Omega} = \left(1 - n - \mu \frac{4R^2}{a_0(a_0+b_0)} \frac{1}{\gamma^2}\right)^{1/2}$$

$$\nu_z \equiv \frac{w_z}{\Omega} = \left(n - \mu \frac{4R^2}{b_0(a_0+b_0)} \frac{1}{\gamma^2}\right)^{1/2}$$

with $\mu = \nu/\gamma = \dfrac{Ne^2}{2\pi R\, m_0 \gamma c^2}$, N total number of electrons in the ring.

4. Parametric Drive of Quadrupole Modes

In the preceding section the quadrupole mode oscillation frequency of a single beam was derived taking into account the collective field of this beam.

In a two beam system this collective field is perturbed by the presence of the second beam. The perturbing frequency is then given by the frequency of beam-beam crossings, which is twice the coherent frequency. It may occur that twice the quadrupole mode frequency matches with the perturbing frequency, in which case resonant growth of the quadrupole mode should be observable (parametric resonance).

For a single beam resonant drive of a quadrupole mode in one phase plane is also possible if in the other phase plane a quadrupole mode is excited with sufficiently strong amplitude. The resonance condition requires that both modes oscillate with the same frequency.

It is a familiar result of parametric resonance theory that the frequency matching condition is weakened with increasing strength of the perturbing force. Besides this it should be also observable that resonant energy transfer to a quadrupole mode occurs if the phase shift with the driving force is close to $\pi/4$.

5. Collective and Single Particle x-z Coupling

As we described in the preceding section density variations in one phase plane may affect quadrupole modes in the other phase plane through the action of collective fields. This is an example for collective x-z coupling, which in general shall be understood as coupling between collective types of motion, i.e. motion for which the phases of individual particles are in some way ordered. Of different nature is the single particle x-z coupling. It may in principle already occur in stationary distributions if the trajectory of a particle in the x-p_x plane depends on its initial conditions in z-p_z.

C Numerical Results

1. Models

Computer calculations were done using the following idealized model of the real physical situation:

a) through a snout at radius r_{sn} relativistic electrons with mass $m_0\gamma$ are injected into a magnetic mirror with field index $n \equiv -\frac{R}{B_z}\frac{\partial B_z}{\partial R}$; they oscillate (coordinates x, z) about an equilibrium orbit with radius R_o and it is assumed that γ, n, R_o are independent of time.

b) transverse collective forces are calculated neglecting radiation effects, image effects and beam curvature. Thus, the total space charge force may be assumed $1/\gamma^2$ times the electric force between charged rods in free space.

Although transverse beam interaction is a two-dimensional problem including x-z coupling, a few important mechanisms may be already investigated in a one-dimensional picture involving only the x-degree of freedom, which shall be described first (for more details see Appendix 1):

1D - BOUNDARY MODEL

In this model the assumption was made that in x-p_x phase space the density within an area representative of the beam is unfiform. A number of particles on the boundary of this area were chosen and their motion calculated by integration of the relevant equations of motion.

The space charge forces acting between particles (rods) were calculated at given time intervals by re-evaluating the phase space figure whose contour can be drawn through the boundary particles, and assuming that the charge density is proportional to the p_x-width of that figure at a given value x.

This way the behaviour of a large number of electrons in the interior of the beam was simulated by using only a small number of particles on the contour and by making use of the properties of phase space representation.

This model was used in sections C.1 and C.3 to demonstrate that quadrupole oscillations and beam-beam energy transfer are essentially 1-dimensional phenomena.

The disadvantage of this model is the occurrence of boundary filamentation (which causes computational problems) and the elimination of x-z-coupling. For this reason a 2-dimensional model following an assembly of macroparticles with x-z coupling was set up (details Appendix 2):

2D - PARTICLE MODEL

At a given cross-section of a beam the transverse forces are calculated as forces between many infinitely long parallel cylindrical rods into which each beam is subdivided. These rods may be considered as "macroparticles" in x-z, carrying a small fraction of the total current. They are injected into the mirror field (linearized about the equilibrium orbit) with arbitrary initial distribution in x-p_x-z-p_z. In section 6) allowance is given for stripping of particles at the injection snout.

In most of the cases the initial distribution COR was applied, in which 144 macroparticles per beam were symmetrically distributed in x-p_x-z-p_z with a correlation such that the total initial energy $E_x + E_z$ was equal for all particles. Only in sections 2) and 6) a distribution UNCOR was used, for which 49 macroparticles were distributed in x-p_x-z-p_z in such a manner that E_x and E_z are uncorrelated. COR is closer to a microcanonical distribution and gives a fairly uniform density. UNCOR has a density with a slight peak in the center and initially rectangular beam cross-section.

Concerning the plots we remark that each macroparticle is labelled by a combination of two numbers or a number and a letter. The print-out indicates the position of the particle centers. If the output points lie closer than the line printer spacing then only the last point is given.

Computer runs were performed with the following parameters, allowing for variations as indicated below

R_o	=	15 cm	(equilibrium radius)
n	=	.4 ... .65	(field index)
γ	=	4	(relativistic mass factor)
j	=	0 ... 600A	(beam current p.turn)
r_{sn}	=	15 ... 18cm	(radial position of injection snout)
d_{sn_x}	=	1.5 cm	(snout diameter in x)
d_{sn_z}	=	1.5 cm	(snout diameter in z)
Δv_x			(initial velocity spread in x)
Δv_z			(initial velocity spread in z)

Unless the contrary is said, Δv_x, Δv_z are chosen such as to have stationary beam cross sections in the absence of space charge.

σ number of particle revolutions
τ number of injected turns

In contrast to a real experiment the injection snout shall not cause particle loss, except in section 6) where optimum conditions for self-inflection are looked at.

The results of computer runs shall be presented in the two phase planes x-v_x and z-v_z, with a scaling for the velocities that makes the initial emittances circular.

2. Quadrupole Modes, Linear and Non-linear Regime

Single beam runs with phase space distributions (referring to the motion relative to the center of mass) that deviate from stationary are shown in fig.1a for the 1D-BOUNDARY MODEL.

These examples were in good qualitative and quantitative agreement with runs using the 2D-PARTICLE MODEL, for which currents in the range of 0 ... 600 A were investigated. We observed that for currents in this range the lowest harmonic of the phase wave (quadrupole mode) was largely dominating for several betatron periods which allows a check of the validity of formula (B.1.1) for the phase wave speed. This shall be done here for the radial mode, where the initial emittance was chosen such that at zero current the beam cross section is exactly stationary.

	j [A]	200	400	600	400 strongly non-stat. emittance
$\nu_{0x} = \sqrt{1-n}$	(n = .55) coherent radial frequency	.67	.67	.67	.67
ν_x	single particle with theor. space charge shift	.55	.44	35	.51
$\bar{\nu}_x$	single particle time-averaged from computer runs	.55	.46	.4	-
a_0	average half radial beam diameter [cm]	.8	.85	.95	1.05
a_1	amplitude of quadrupole oscillation [cm]	.05	.1	.15	.55
$\alpha/\nu_x = \frac{\nu_x' - \nu_x}{\nu_x}$	theor. relative shift of mode frequency	.091	.25	.50	-
$\alpha/\bar{\nu}_x$	computational relative shift of mode frequency	.091	.15	.25	-
ν_x'	computational mode frequency	.60	.53	.50	.57

Table 1. Quadrupole modes for 2D-PARTICLE MODEL

We observe good agreement of the theoretical and computational values for $\alpha/\bar{\nu}_x$ for small amplitude modes. For larger amplitudes the theoretical values are too high, as one should expect.

ν_x was theoretically determined from (B.1.2) with an averaged value for a_o, b_o taken from computer runs.

The theoretical and the computational values for the single particle frequency (ν_x and $\bar{\nu}_x$) differ for increasing current. This is due to the fact that the phase velocity of particles oscillates with the frequency of boundary oscillations. The time-averaged value $\bar{\nu}_x$ then shows less space charge influence than the theoretical ν_x determined from a corresponding stationary distribution (obtained by time-avering the dimensions of the fluctuating beam).

The qualitative features of phase wave propagation in the non-linear regime (large amplitude mode, $a_1 \not\ll a_o$) are displayed in fig.2 for a run with 400 A, n = .55 and an initial radial emittance, which was stretched in p_x and compressed in x by a factor of 2. We observe the following characteristics (for the motion relative to the c.o.m.):

a) single particles rotate in x-p_x with strongly oscillating phase velocities. Already during the second phase revolution the boundary ellipse starts developing tails, which are slightly accelerated compared with the main body of the distribution. Particles with large initial amplitude and favorable phase are locked in the tails and rotate with the mode frequency .

b) the relative shift α/ν of mode frequency is less than for small amplitude modes, where it was independent from the amplitude a_1.

Maximum aplitude particles locked in tails may be in resonance with the mode frequency ν_x' for many periods. They can be driven then to still larger amplitudes and disintegrated from the bulk of the distribution.

In addition to this we found a change in amplitude of the axial quadrupole mode. From an initial value of .1 cm it grew to approximately .3 cm within the first two betatron periods. During this time the z-phase wave was on the average 45° ahead of the x-phase wave, which favoured parametric amplification of the z-mode due to the dependence of the axial space charge force on the radial beam dimension. The same run with small initial radial mode amplitude has not shown such x-z-coupling, because ν_x' was not close enough to ν_z' (linear regime for the mode frequencies) and the variation in radial beam dimension (which gave the strength of the driving force) was too small.

The parametric action of a large amplitude quadrupole mode in one degree of freedom on a quadrupole mode in the other degree of freedom is an example of intra-beam collective coupling via electromagnetic fields. Independent hereof is the single particle coupling which shall be discussed in the next section.

3. Single Particle x-z Coupling

Single beam runs with 200 A were done at n = .5 (fig.3) and n = .55 with the 2D-PARTICLE MODEL and initial distribution UNCOR. The density being slightly peaked in the center of the beam, some coupling between x and z was expected in this case and we observe the following characterisitics:

a) phase slip; particles with equal initial position in x-p_x but different amplitudes in z-p_z show after some time a phase slip, which is maximum for vanishing z-amplitude. This reflects the fact that the x space charge force averaged over the radial extent of the beam is maximum at z = 0.

b) x-z energy exchange; particles, whose phase angles in x-p_x and z-p_z differ by an amount close to 90° exchange energy between both degrees of freedom if the field index n equals .5. In this case the amount of energy exchange is of the order of 5% per phase revolution, whereas n = .55 shows no directed energy exchange.

4. Beam-beam Energy Transfer and Self-inflection

With an initial coherent x-amplitude (R = 15 cm, r_{sn} = 16 or 17 cm) the energy transfer between two sequentially injected beams as well as the distortion of individual beam's phase space areas is shown in runs with 200 and 400 A at different n-values.

<u>1D - BOUNDARY MODEL: j = 200 A; r_{sn} = 16 cm; n = .55</u>

An extra distortion of the phase space areas visible after one revolution comes from the external force which was not chosen harmonic in this model and leads in the x-p_x plane to a slight acceleration of particles with larger amplitude (fig.1b).

<u>2D - PARTICLE MODEL: j = 200, 400 A; r_{sn} = 17, 16 cm;</u>

400 A (n = .55)

after two betatron periods of interaction of the first and second turn the amplitude of the c.o.m. of the first turn was reduced by a factor 1.72 and for the second turn was increased by a factor 1.22. The phase angle between the two turns remained nearly unchanged (i.e. 120° degrees), whereas they both lagged in phase by 30° (compared with zero current). This corresponds to a reduction of the coherent radial betatron frequency of ~ 4% due to beam interaction (fig.5).

200 A (n = .55)

the exchange of energy and the phase lag where half of the full current values.

400 A (n = .45)

after two betatron periods of interaction the amplitude of the c.o.m. of the first turn was reduced by a factor 2.16 and for the second turn increased by 1.26 with a practically unchanged phase angle between the turns (fig.6).

n = .4 (400 A)

after two betatron periods of interaction the c.o.m. amplitude of the first turn was reduced by a factor of 2.4 and for the second turn increased by a factor of 1.28. The phase angle between the two turns (initially 81°) was gradually decreasing.

n = .4 (500 A)
the energy transfer during the first two betatron periods is stronger than before, but during the third period it stops because the phase difference between the turns gets zero.

The general conclusion for the influence of the field index n on self-inflection is the following: The (initial) energy exchange between the turns is more intensive if the phase angle between them is small. As soon as they have very different coherent amplitudes their phase difference becomes unstable; it decreases (and reverses sign) if it was initially substantially less than 90°. At zero phase difference energy transfer (per betatron period) is zero and changes its direction. This shows that for optimum energy exchange a phase difference of about 90° is most favorable because of its good stability.

We remark that with the amplitudes of coherent motion obtained after two betatron periods the total energy in coherent motion is slightly reduced. This defect in energy apparently is related to the excitation of a quadrupole z-mode (to be studied in section 4).

The lowering of the coherent amplitude of one beam by beam-beam interaction opens the possibility of self-inflection, which will be discussed more extensively in section 6).

For 1 cm coherent amplitude (r_{sn} = 16 cm) beam-beam interaction assumes a pronounced nonlinear character which results in distortion of the phase space areas for high current. This behaviour is unfavorable to energy exchange. See fig.7 for the 2D-PARTICLE MODEL and fig.1b for the 1D-BOUNDARY MODEL.

5. Parametric Drive of Quadrupole z-Mode - Two Beams

Two 400 A beams were sequentially injected 2 cm off from equilibrium radius. n varied between .45 ... .65 and the initial distribution COR was chosen.

Fig.8 shows a parametric drive of a z-quadrupole mode for either beam. At n slightly larger than .5 the frequency of subsequent x-crossings of the beams is expected to be twice the z-quadrupole mode frequency which yields optimum resonance conditions. Accordingly the n = .55 run shows maximum growth of the mode amplitude, which is doubled within approximately four revolutions of the second beam.

At n = .45 no noticeable growth of the z-quadrupole mode was observed; at n = .65 a slight growth occurred. At n = .45 in fact the z-mode frequency is too low to match with the driving frequeny, whereas at n = .65 a high enough current can in principle give matching of frequencies if the space charge shift is taken into account.

For 200 A beams (at n = .55) the effect was reduced according to the lowered driving force which results in about half the growth of amplitude compared with 400 A.

At small coherent x-amplitudes the nonlinear character of beam-beam interaction mismatches the resonance condition and there is no pure quadrupole mode growing (see fig.8d).

6. Parametric Drive of Quadrupole x-Mode - Two Beams

The same mechanism leading to amplification of a quadrupole z-mode may in principle also drive a quadrupole x-mode. In fact the run with n = .45/j = 400 A mentioned in the preceding section showed growth of this mode by a factor of 1.5 during the first three revolutions of the second beam (fig.6). At n = .55 (fig.5) and more evidently at n = .65 no particular growth of the x-mode was observed.

In view of our theoretical understanding this behaviour should be looked at in the following way:

In order that growth of an x-mode can occur its frequency (in phase space) must be close to half the driving frequency. An initial phase relation between driving force and mode can thus be maintained for at least several mode periods. If in addition the initial phase difference was such that energy transfer to the mode is favoured ($\Delta\varphi \simeq \pi/4$), we may expect a net growth of amplitude during only few periods of the mode.

The latter requirement is demonstrated in a comparative run (n = .45/j = 400 A), where the initial ellipse in x-p_x was rotated by 90°. In this case practically no growth of the x-mode amplitude was observable, although the frequencies matched well.

Phase and frequency of the driving force result from the combined effects of radial beam crossings and of oscillations of the axial beam width. If the amplitude of axial oscillations is large as in the case n = .55 where parametric excitation occurred, they may shift the phase of the resultant driving force and thus destroy the growth conditions for the radial mode. This effect should contribute to the case n = .55 where nearly no growth in the amplitude of the radial mode was observable.

At n = .65 mismatching of frequencies can easily be identified as the reason why no growth of the radial mode occurred.

For weaker current - where the resonance condition is satisfied even more accurately - amplification of the radial mode is lowered according to the weaker driving force.

7. Self-inflection in Multi-beam Systems

To establish optimum conditions for self-inflection within the framework of the present model several principles have to be taken into account. These principles also have an important bearing on active inflection, which they may alter substantially in many cases if the current is high enough.

a) Beam-beam energy transfer is most favorable if the initial phase difference between the beams is about 90°.
b) Axial growth of the beams due to parametric excitation can be avoided if $n < .5$. This favours on the other hand radial growth of the beams which, however, is less harmful to the holding power than the observed axial growth.

In the following the initial distribution COR with 49 macroparticles per beam is used and allowance is given for particle stripping at the injection snout.

Two-beam system:

It is clear from above observations that a two-beam system can at most achieve self-inflection of one beam (the first beam, unless $n > .75$, where the situation reverses).

Optimum self-inflection ($\sim$ 70% of the first beam) was obtained computationally at n = .4 or .45 (j = 400 A, r_{sn} = 17 cm), see fig.8. Complete inflection of the first turn failed because of the large quadrupole oscillation amplitude of the beam (parametric effect) during the fourth and most dangerous passage at the snout, which indicates that higher current cannot increase the rate of inflected current.

At larger distance snout-equilibrium radius (r_{sn} = 18 cm, n = .4, j = 400 A, (see fig.9)) energy transfer was too weak. Although 60% of the first beam was saved after the fourth revolution, it had a coherent amplitude of 2 cm. This shows that the snout should be so close to the equilibrium orbit as to just leave enough space for the (inflected) beam to pass - of course taking into account the growth it experienced owing to space charge and parametric effects.

Three-beam system:

With about 90° phase difference between the beams (n = .4, .45, fig.10) the first injected beam lost energy as in the corresponding two-beam system. It transferred energy to the second beam, which gave nearly all gained energy to the third beam. Therefore, the first beam could again be well inflected (to 75%), whereas the third beam was lost and a small part (30%) of the second beam was trapped at a coherent amplitude of $\sim$ 1 cm.

With 120° phase difference (n = .55,fig.11) between the beams the distribution in x-p_x has the highest symmetry, which is most unfavorable to energy exchange. Neither beam is well inflected, but only fractions of each beam are trapped at amplitudes of $\sim$ 1 cm. This trapping is possible owing to the growth of the x-quadrupole mode.

The number of beams in the system effects upon the occurrence of parametrically driven x- or z-quadrupole modes. In the presence of two further beams each beam suffers four beam-crossings per betatron period. These crossings in general do not occur at equal time intervals. Therefore the perturbing force resulting from them is very unlikely to act on the modes in a resonant way. Instead of growing amplitudes of pure quadrupole modes as in the (resonant) two-beam system we obtained rather incoherent beam growth in x or z respectively. This leads, however, to a similar weakening of the holding power (when comparing two- and three-beam systems with equal current per beam).

For systems with a higher number of beams a similar arguing holds and one can easily derive qualitative features of the self-inflection mechanism.

In an active inflection-system one might be interested in reducing self-inflection effects. With the foregoing observations this should be possible to some extent by a convenient choice of n for a given number of beams.

The 400 A current per beam used in the examples of this section was optimum in the sense that higher injected current did not increase the rate of inflected current. This expresses the self-limiting nature of self-inflection.

D Conclusion

Transverse collective interaction of relativistic electron beams in magnetic mirrors has been studied using a numerical model with interacting macroparticles. It was found that collective interaction may substantially alter the distribution of particles in phase space. The main consequences of this interaction were:

(1) energy transfer between beams affecting their c.o.m. motion; the amount of exchanged energy depends on the phase shift between the beams.
(2) energy transfer between the c.o.m. motion of one beam to a quadrupole mode of another beam; if phase and frequency of the c.o.m. motion and quadrupole mode are in resonance condition, resonant energy transfer is possible.
(3) energy transfer between quadrupole modes of one beam in either degree of freedom; again resonant energy transfer is possible.

In practice these modes of interaction do not occur separately, which makes the picture more complicated because of their mutual perturbation.

The quantitative features of beam-beam and intra-beam interaction depend on the beam current,current density and the time available for interaction. The current range investigated here (200 - 400 A per beam) was intermediate in the following sense: for less current the interaction-induced change in beam quality observable after typically five particle revolutions is a minor effect. For higher current and all other parameters unchanged, interaction assumes strongly nonlinear features which may result in rapid filamentation and an increase of effective phase space. Thus space charge density gets more stationary and transverse interaction effects saturate, of course on the cost of bad beam quality. This shows the self-limiting nature of the transverse collective effects studied here.

Acknowledgements

The authors wish to thank E. Springmann for the computer program of the 2 D PARTICLE MODEL and Mrs. K. Klug for typing the manuscript.

Bibliography

1. D.W. Kerst, Phys.Rev.74, 503 (1948)

2. I.M. Samoilov and A.A. Sokolov, Zh.Eksperim.i Teov.Fiz.39, 257 (1960) Engl.transl.: Soviet Phys. - JETP 12, 185 (1961)

3. C. Andelfinger, Particle Accelerators 5, 105 (1973)

4. I.N. Ivanov et.al. JINR Report P 9 - 4132 (1968)

5. L.J. Laslett, ERAN 30 (1969), Lawrence Radiation Lab., Berkeley (unpublished)

6. M. Reiser, Particle Accelerators 4, 239 (1973)

7. L.J. Laslett, ERAN 44 (1969)

8. L. Collatz, The Numerical Treatment of Differential Equations, Springer (1969), p.69

Appendix 1: 1D BOUNDARY MODEL

a) Space Charge Forces

Since in this mode the x-z coupling was not considered, assume that, in real space, the beam has constant z-width w.
Slice the beam in ribbons of width w and thickness dR in radial direction. If   is the charge per unit length of the beam at the ribbon, under the assumption that the charge density in phase space is constant, it is

$$\lambda = \frac{j}{\beta c} \; \frac{u(R)\, dR}{S} \tag{1}$$

j is beam current, u the width of a slice of the phase space beam area, S this area.

To calculate the space charge forces due to a ribbon on an electron in P at a distance R, slice each ribbon lengthwise into wires of cross section dR.dZ and add up all the contributions in P, by taking only the radial component of the electric force and introducing a factor $(1 - \beta^2)$ to allow for the partial cancellation of electric and magnetic forces. Moreover, average over all z-positions of electrons in the beam. The radial space charge force per unit rest mass is then

$$\begin{aligned} f_x &= \frac{2e\,(1-\beta^2)}{m_0 \beta c} \; \frac{j}{S w^2} \int dR\, u(R) \int dz \int dZ \, \frac{R}{R^2+(Z-z)^2} \\ &= \frac{2e}{\gamma^2 m_0 \beta c} \; \frac{j}{S w} \int dR\, u(R) \left[2 \arctan \frac{w}{R} - \frac{R}{w} \ln\left(1+\frac{w^2}{R^2}\right) \right] \end{aligned} \tag{2}$$

b) Equations of Motion

The relativistic equations of motion in this one-dimensional case can be written (v_x radial velocity component):

(3)

$$\frac{dv_x}{dt} = \beta\omega + \frac{1}{\gamma}\left(1 - v_x^2\right)f_r + \frac{\beta c}{r}$$

$$\frac{dx}{dt} = c v_x \,, \qquad \omega = \frac{e}{m\gamma} B_z$$

The term $\beta\omega$ represents the external forces acting on the beam. The guide field was expressed as

(4) $$B_z = B_0 \left(1 + \frac{x}{R}\right)^{-n}$$

with constant field index n.

c) Beam-beam Interaction

The same (2) was used for the space charge forces. Only the integrals in R and Z were extended over both beams.

d) Computational Procedure

Take N electrons on the boundary of an initial phase space ellipse. Integrate the equations of motion (3) for each particle. After a (short) time interval draw the new phase space boundary through the new coordinates of the particles and re-calculate the space charge forces by means of (2).

A check made on the phase space figure has shown that the area S remains constant for several phase space revolutions within 1.5%, in a typical run with N = 12 electrons and boundary re-evaluation after every 5^o in phase space. This result was encouraging for the use of such a small particle number and the resulting very short computer time.

The computation, performed on the IBM 360/91 of the IPP Institute in Garching, made use for the integration of the IBM-SSP predictor corrector routine HPCG.

<u>Parameters for the Computation</u>

electron kinetic energy	= 2 MeV
equilibrium radius	= 15 cm
injection radius	= 16 cm
initial phase - space area (emittance)	.75 cm x 30 mrad
field index	= .55
beam current	0 - 400 A
beam size in z	= 1 cm
No. of boundary electrons	12 - 16
ribbon thickness	= .1 cm

Appendix 2: 2D-PARTICLE MODEL

a) Equations of Motion for Macroparticles

The relativistic equations of motion for small oscillations of an electron about an equilibrium orbit R_o in a magnetic mirror with field index n are:

$$\text{(1)} \quad \frac{dv_x}{dt} + \omega_0^2(1-n)\,x = \frac{e}{m_0\gamma}\left(E_x^s(x,z) + \beta B_z^s(x,z)\right)$$

$$\text{(2)} \quad \frac{dv_z}{dt} + \omega_0^2\, n\, z = \frac{e}{m_0\gamma}\left(E_z^s(x,z) - \beta B_x^s(x,z)\right)$$

For the numerical treatment each beam is represented as an assembly of N straight parallel cylindrical rods, each carrying a fraction (j/N) of the total charge and current. The motion of each rod, called macroparticle, obeys (1), (2), with the electric and magnetic self-fields E^s, B^s computed as sums of interaction forces with all other macroparticles. This procedure is convenient for the present study of such collective phenomena which show their characteristic features already at a relatively low number of macroparticles.

If the radius of a macroparticle is ρ and its charge per unit length λ, the repulsive force between two of them is a function of the distance s of their centers. One can easily compute the force between a macroparticle of radius ρ and one of zero radius, both carrying equal line charge λ:

$$f = \begin{cases} \dfrac{1}{\gamma^2}\dfrac{2\lambda^2}{s} & s > \rho \\[2ex] \dfrac{1}{\gamma^2}\dfrac{2\lambda^2}{\rho^2}\, s & s < \rho \end{cases}$$

If both macroparticles have radius ρ the interaction force is weakened in the range $s < 2\rho$ because of the partially overlapping charges. The following formula yields a good approximation for the correct force:

$$f = \frac{1}{\gamma^2}\frac{2\lambda^2}{\rho^2 + s^2}\, s \qquad (0 < s < \infty)$$

The total self-force on a macroparticle is then

$$F_x^s = \frac{2\lambda^2}{\gamma^2} \sum_j \frac{x - x_j}{\rho^2 + (x-x_j)^2 + (z-z_j)^2} = \lambda \left(E_x^s + \beta B_z^s \right) \tag{3}$$

$$F_z^s = \frac{2\lambda^2}{\gamma^2} \sum_j \frac{z - z_j}{\rho^2 + (x-x_j)^2 + (z-z_j)^2} = \lambda \left(E_z^s - \beta B_x^s \right) \tag{4}$$

As follows from the definition of this force, it includes only interaction between near-by particles, i.e. all particles staying at the same azimuth.

b) Computational Procedure and Initial Distributions

Trajectories of macroparticles are computed by solving (1), (2) using an improved polygon method [8)] with recalculation of (3), (4) at each integration step.

For our purpose it is convenient to distribute the initial conditions for the macroparticles of one beam as symmetrically as possible in phase space in order to get smooth space charge densities. This is realized in two different distributions which are obtained in the following way:

(1) COR consists of 2 x 72 particles: six (twelve) points symmetrically placed on a circle of radius 1/2 (1) in the x-v_x plane are combined with twelve (six) points symmetrically placed on a circle of radius 1 (1/2) in the z-v_z plane.

(2) UNCOR consists of 7^2 particles: six points on the unit circle and one in the center of each phase plane are combined with each other.

The x and z widths of the distributions are adapted to the injection snout aperture, whereas the v_x and v_z widths are chosen so that the resulting emittances are stationary with absence of space charge effects (except fig.2).

Sequentially injected turns start with the same initial conditions. Electrons at a given cross section of one turn are allowed to interact with those electrons of all other turns that stay at the same azimuth.

The radius of macroparticles is chosen just so small that in the initial x-z-projection no overlapping of particles occurs.

Figures

fig.1: Computational results for 1 D-BOUNDARY MODEL

fig.2 - 12: Computational results for 2 D-PARTICLE MODEL

(phase space representations)

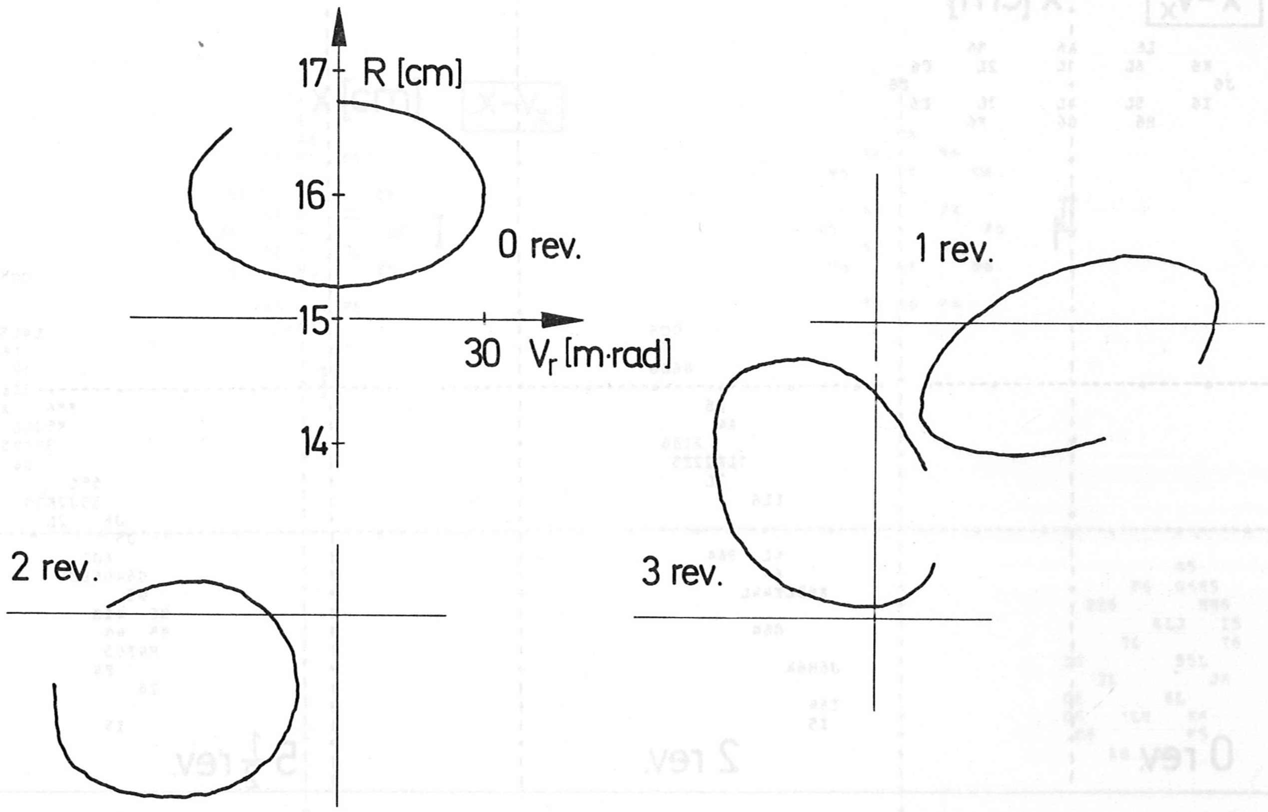

fig. 1a x-quadrapole oscillation n=.55 j=200 A r_{sn}=16cm one beam 1D BOUNDARY MODEL

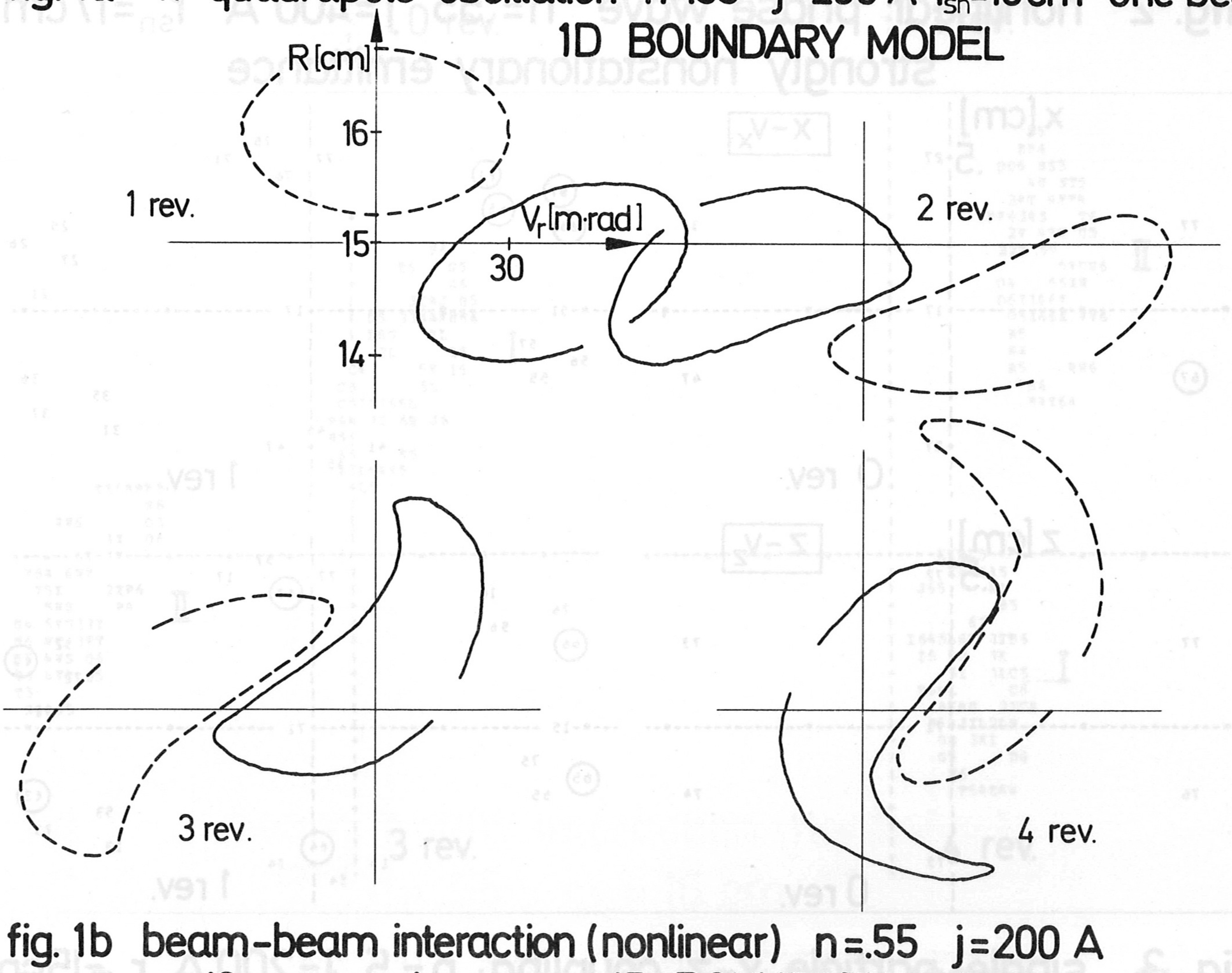

fig. 1b beam-beam interaction (nonlinear) n=.55 j=200 A r_{sn}=16cm two beams 1D BOUNDARY MODEL

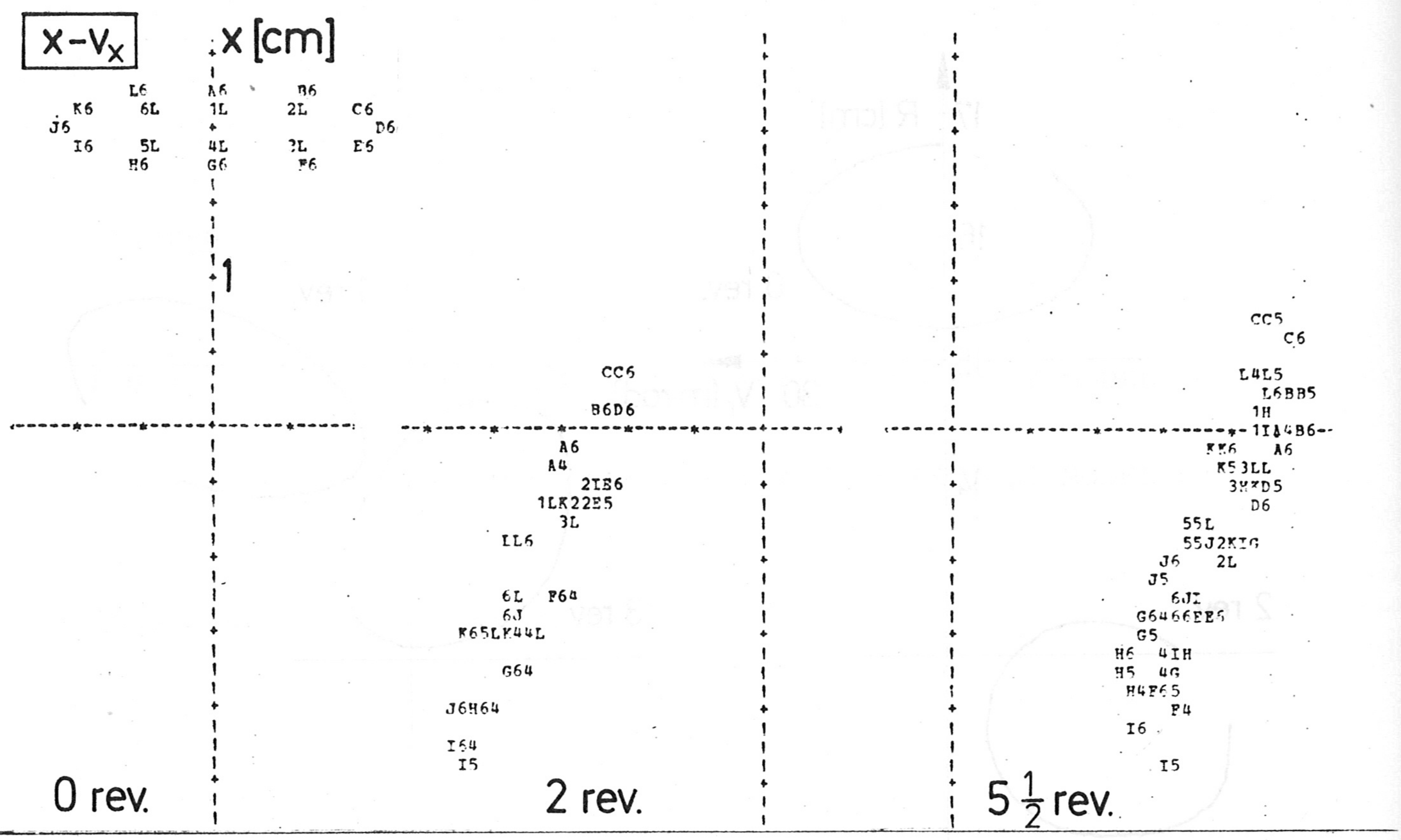

fig. 2 nonlinear phase wave n=.55 j=400 A r_{sn}=17 cm
strongly nonstationary emittance

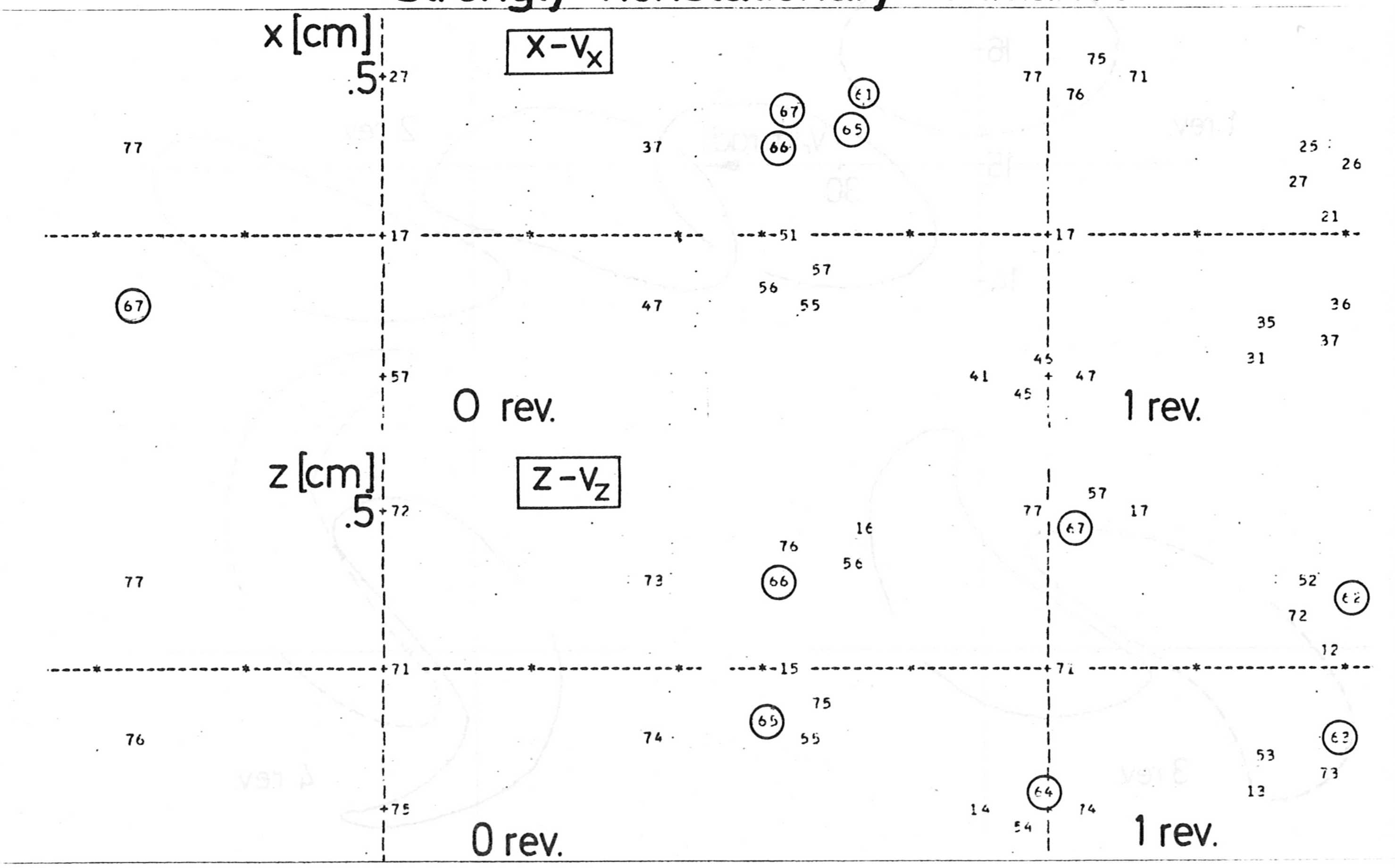

fig. 3 single particle x-z coupling n=.5 j=200 A r_{sn}=15 cm
(stretched in v_x , v_z)

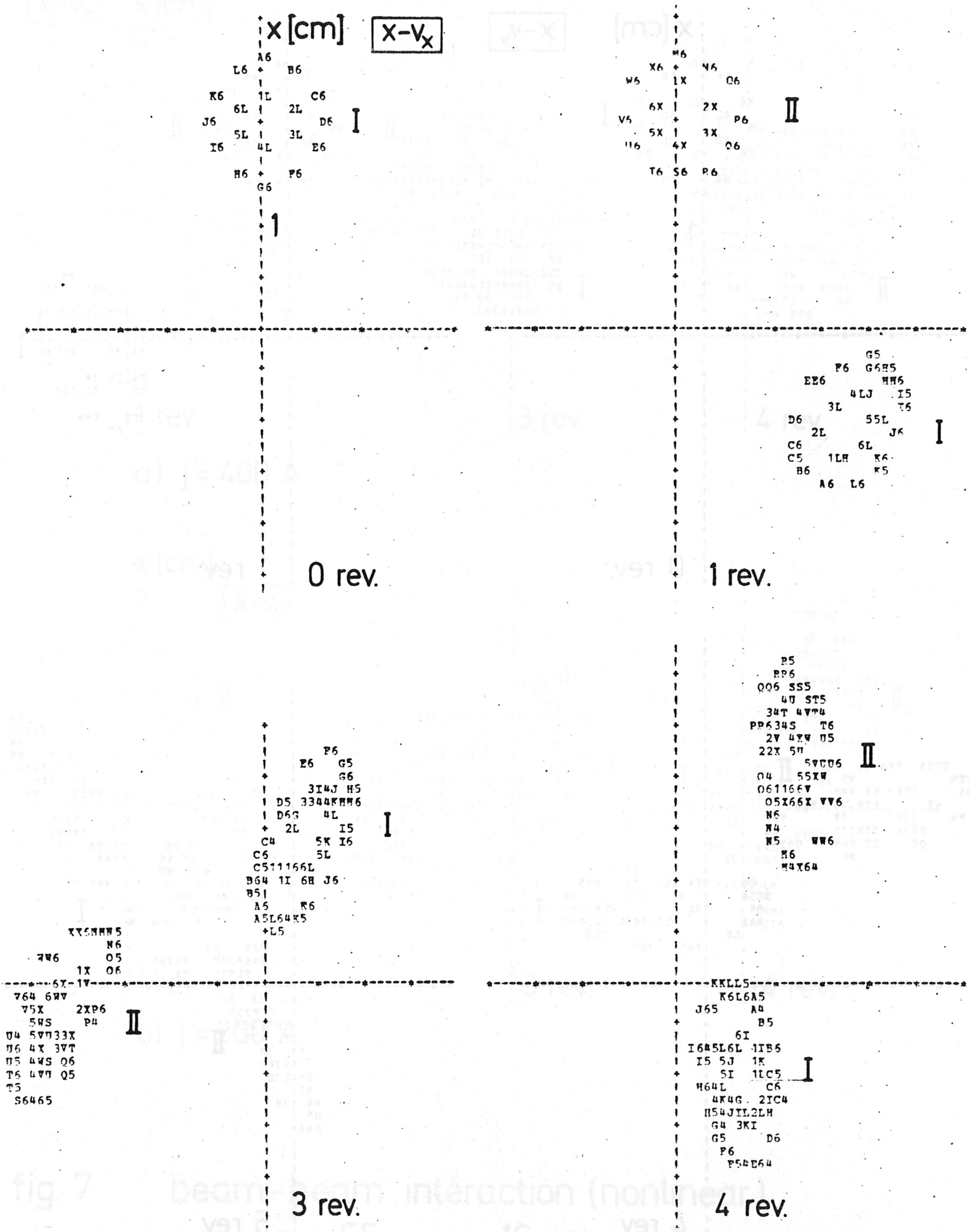

fig. 5 beam-beam interaction n=.55 j=400 A r_{sn} = 17 cm

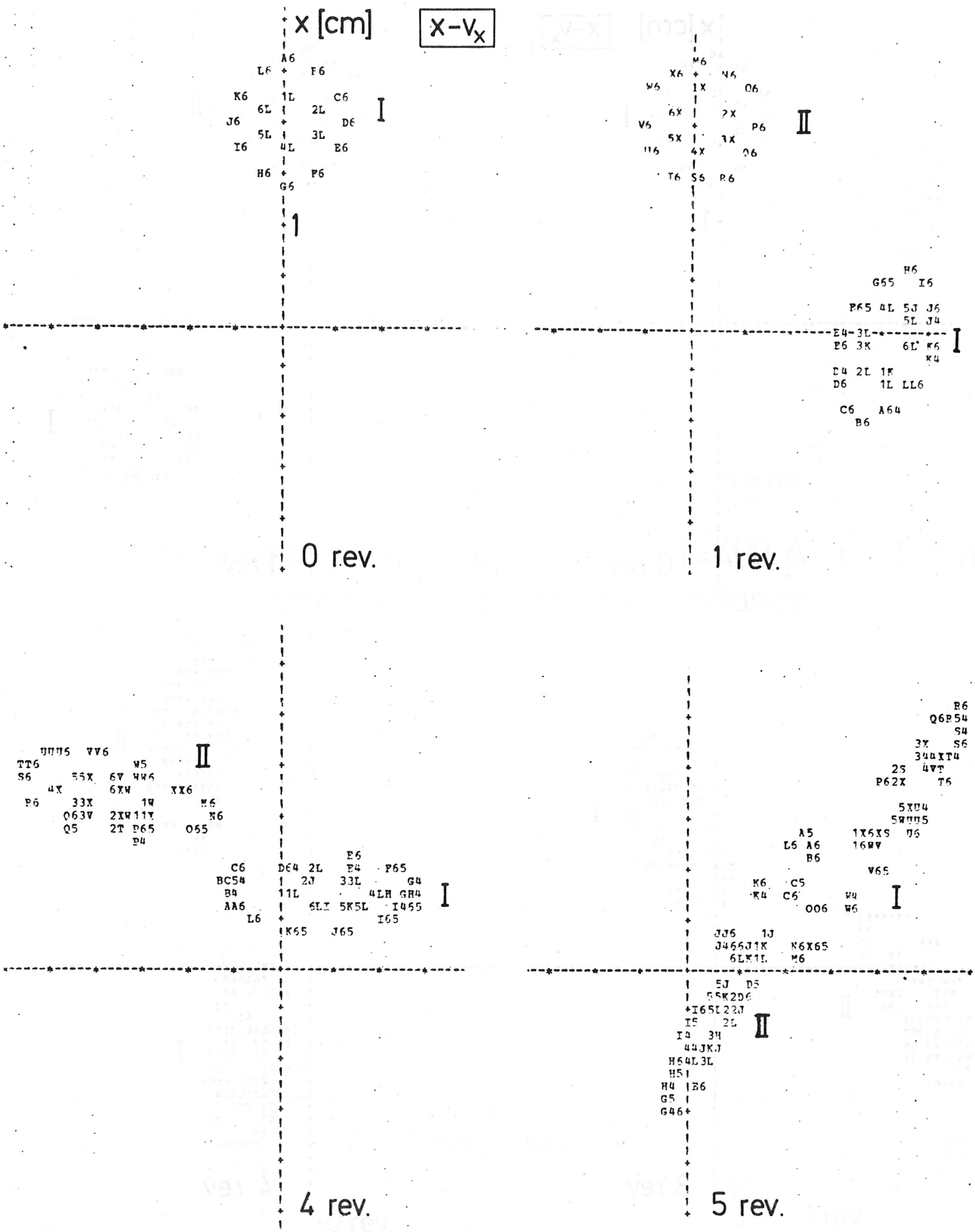

fig. 6 beam - beam interaction n = .45

$j = 400$ A $r_{sn} = 17$ cm

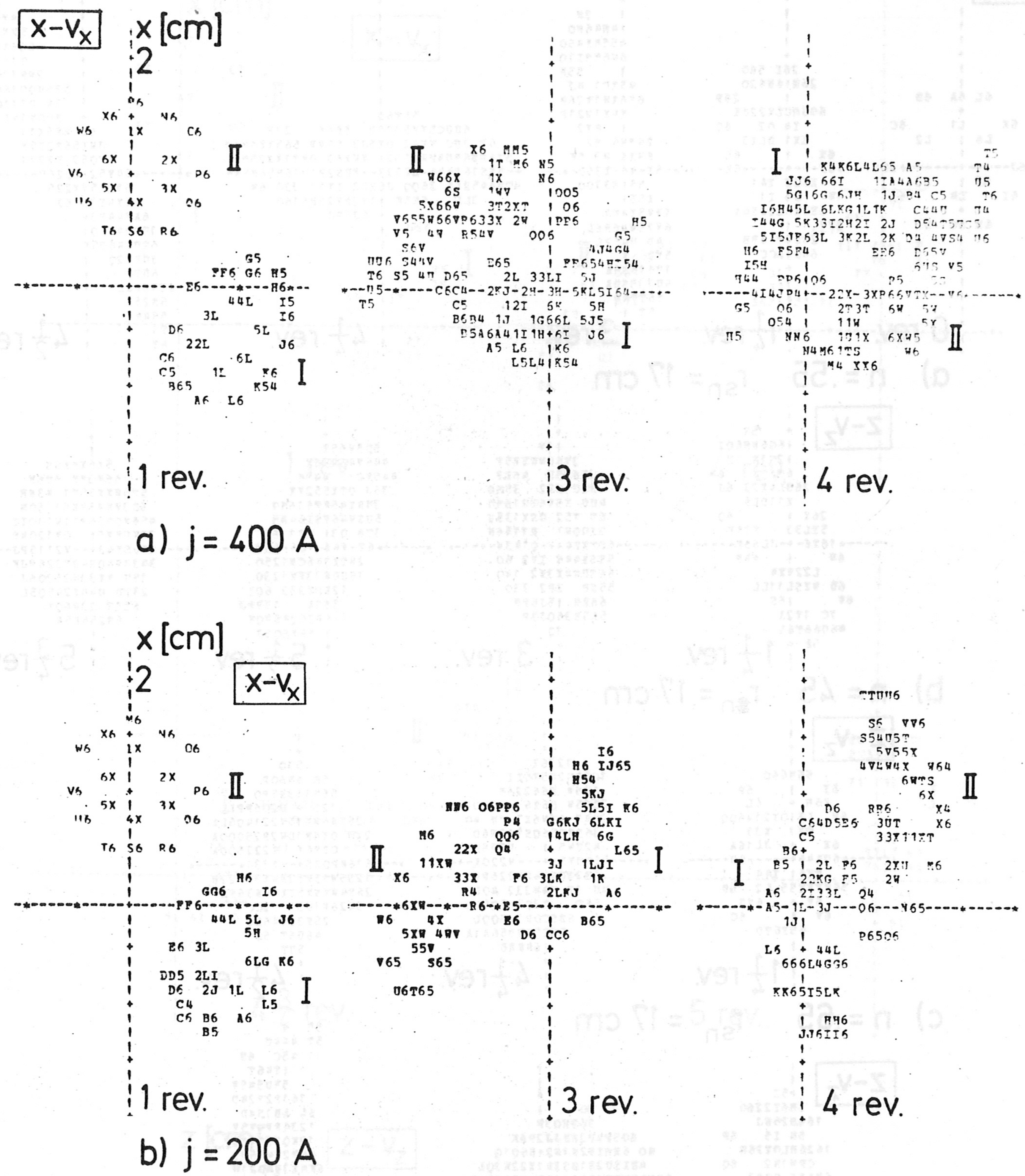

fig. 7 beam-beam interaction (nonlinear)

$n = .55 \quad r_{sn} = 16$ cm

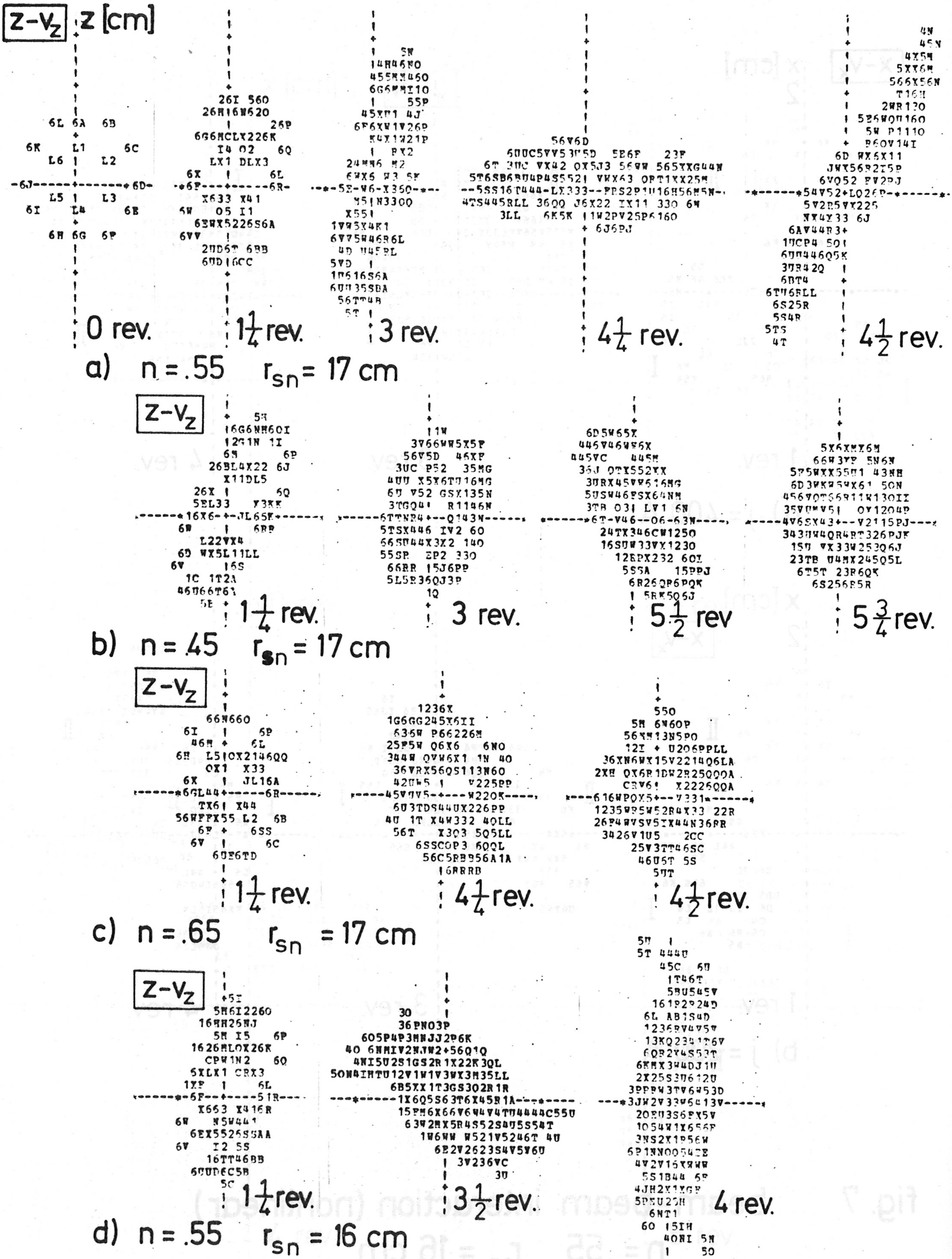

fig. 8 parametric drive of quadrapole z-mode j=400 A
two beams

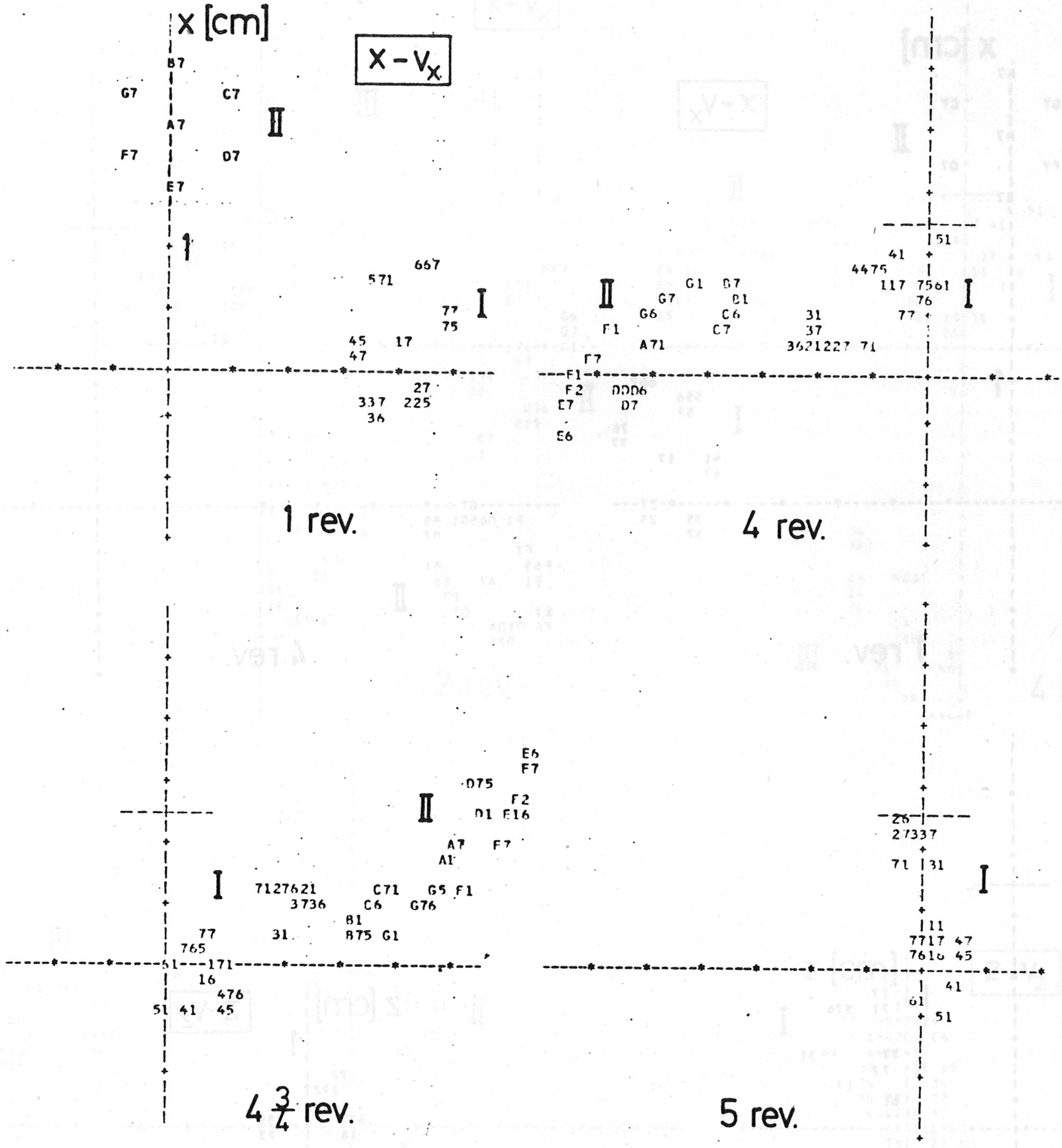

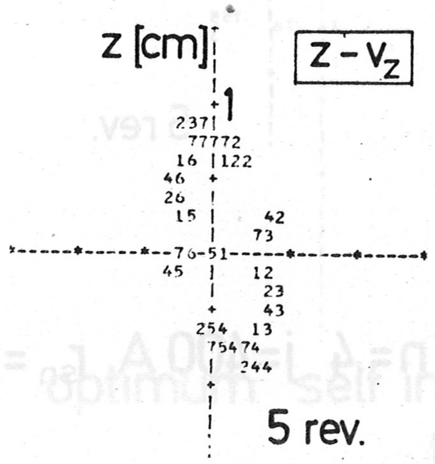

fig. 9
optimum self - inflection
n=.4 j=400 A r_{sn} =17 cm
two beams

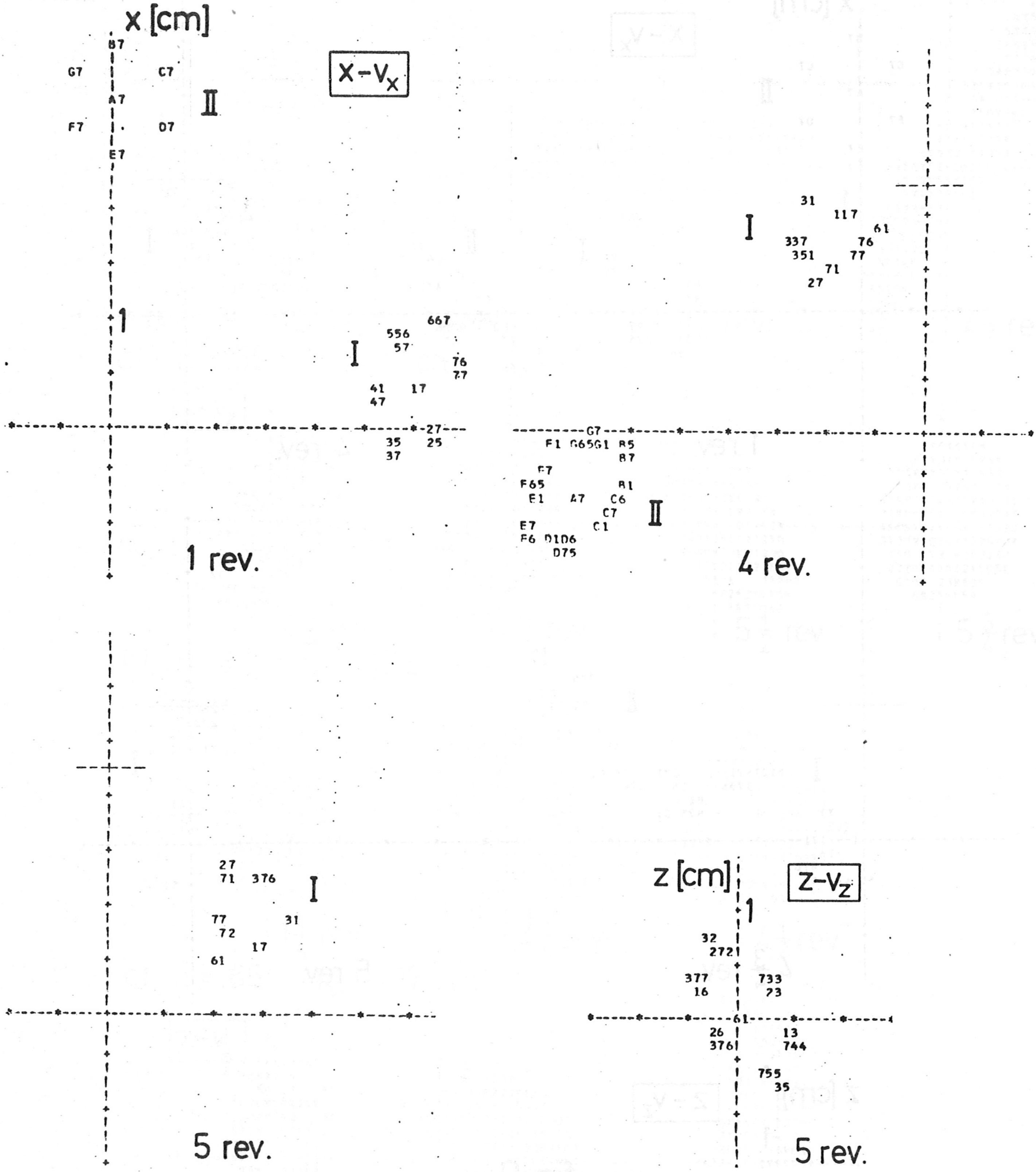

fig. 10 optimum self - inflection $n=.4$ $j=400\ A$ $r_{sn}=18\ cm$
two beams

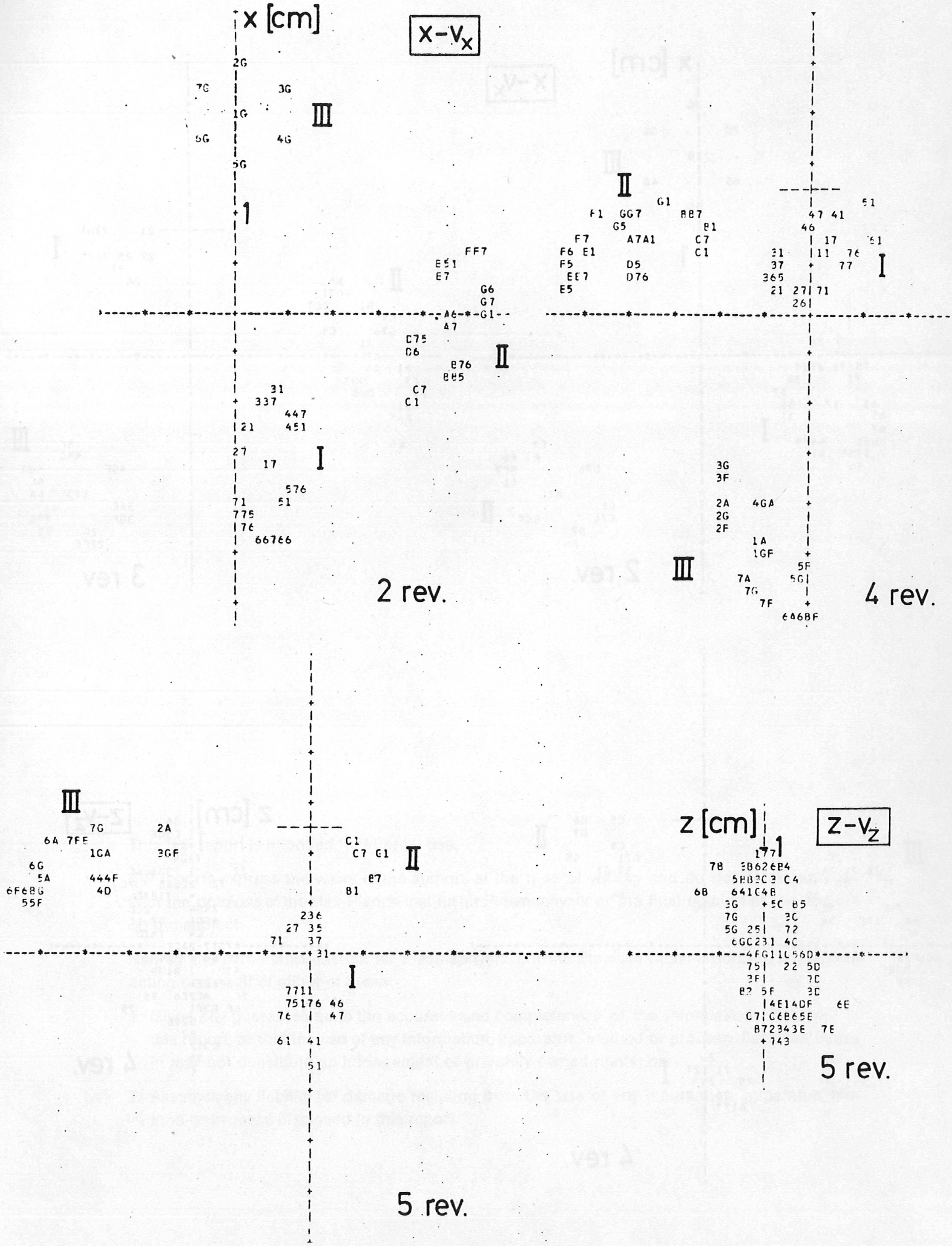

fig. 11 optimum self inflection $n=.4$ $j=400\ A$ $r_{sn}=17\ cm$
three beams

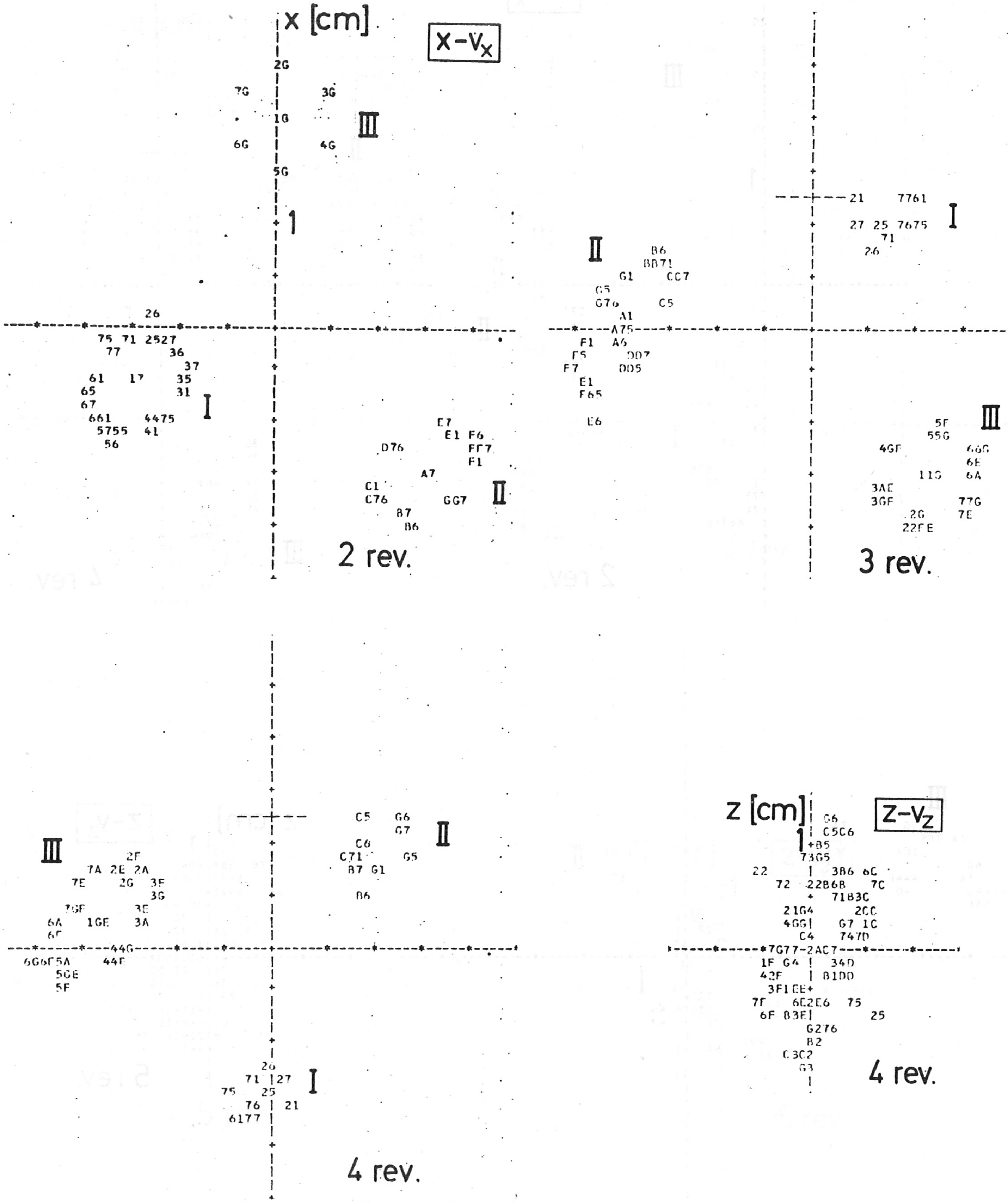

fig. 12 optimum self inflection $n=.55$ $j=400\,A$ $r_{sn}=17\,cm$
three beams